

# Robust Neural Control of Wind Turbine Based Doubly Fed Induction Generator and NPC Three Level Inverter

Khadraoua Narimene<sup>1\*</sup>, Mendaz Kheira<sup>2</sup>, Flitti Mohamed<sup>3</sup>

<sup>1</sup> SSL Laboratory, Department of Electrical Engineering, University Belhadj Bouchaib Ain Temouchent, 46000 Ain Temouchent, N101 Route de Sidi Bel Abess, Algeria

<sup>2</sup> RECOM Laboratory, Department of Electrical Engineering, University Belhadj Bouchaib Ain Temouchent, 46000 Ain Temouchent, N101 Route de Sidi Bel Abess, Algeria

<sup>3</sup> ICEPS Laboratory, Department of Electrical Engineering, University Belhadj Bouchaib Ain Temouchent, 46000 Ain Temouchent, N101 Route de Sidi Bel Abess, Algeria

\* Corresponding author, e-mail: [khadraoua21@gmail.com](mailto:khadraoua21@gmail.com)

Received: 27 January 2022, Accepted: 05 April 2022, Published online: 16 May 2022

## Abstract

This paper presents dynamic modeling and control of Doubly Fed Induction Generator (DFIG) based on wind turbine systems, where the stator of DFIG is directly connected to the grid and the rotor was fed by a three level PWM NPC inverter. The active and reactive power control of the DFIG is based on the feedback technique by vector control method by using a classical regulator of Proportional-Integral (PI) type which allows us, in association with the looping of powers, to obtain an efficient and robust system. This approach is a very attractive solution for devices using DFIG as wind energy conversion systems; because, it is a simple, practical implementation, commonly applied in the wind turbine industry and it presents very acceptable performance, However, this control approach has certain limitations and has several causes, vector command with NPC three-level inverter pulse width modulation (PWM) is used to control the reactive power and active power of the generator. Then, use the neural network design to replace the traditional proportional-integral (PI) controller. Finally, the Matlab/Simulink software is used for simulation to prove the effectiveness of the command strategy.

## Keywords

DFIG, three level NPC inverter, active power control, vector control, Proportional-Integral (PI), Artificial Neural Network

## 1 Introduction

Renewable energy sources such as solar, wind, sea energy (tidal and wave) and biomass emerged as a solution for global warming effect, population growth, fossil-fuel depletion and its insecure transportation. Wind energy is one of the most important and promising sources of renewable energy all over the world, mainly because it reduces the environmental pollution caused by traditional power plants as well as the dependence on fossil fuel, which have limited reserves [1, 2].

Wind turbines are largely deployed due to their variable speed feature and hence influencing system dynamics. But unbalances in wind energy are highly impacting the energy conversion and this problem can be overcome by using a Doubly Fed Induction Generator (DFIG) [3–7]. Doubly fed wound rotor induction machine with vector control is very attractive to the high-performance variable speed drive and generating applications. The DFIG used

in several wind energy conversion systems. This machine has proved its efficiency due to qualities such as robustness, cost and simplicity. It offers several advantages, including variable speed operation.

The vector control (more specifically the one with orientation of the stator flux) will allow us to realize a control independent of the active and reactive power of the DFIG, by using classical regulators of Proportional-Integral (PI) type [8].

The purpose of the vector control is to control the DFIG as an independently excited direct current machine where there is a natural decoupling between the magnitude controlling the flux (the excitation current) and that related to the torque (the armature current) [9–11].

The proportional integral active reactive power control is a very attractive solution for devices using DFIG

as wind energy conversion systems; because, it is a simple practical implementation, commonly applied in the wind turbine industry and it presents very acceptable performance [11–14]. However, this control approach has certain limitations and has several causes. As example, its performance mainly counts on the PI controller design mode and the exactitude in DFIG-generator parameters and the connected electric power grid voltage conditions.

The Artificial Neural Network (ANN) is widely used as a universal approximates in nonlinear mapping and uncertain nonlinear control problems. Artificial neural control is very powerful tool capable of achieving very good results in the control of complex systems. It is preferred to use Artificial Neural Networks (ANN) for control when requirements for precision are high and system is not identified precisely, or its parameters are changing [3–17].

The used of Neural Network (NN) in the DFIG system to reduce system parameter ripples and harmonic distortion of the rotor current. The stator active and reactive power were controlled using both neural and PI approaches for determining the sensitivity to uncertainties

In the new universal grid code for wind power generation, the power quality of wind energy is included [11]. For this reason, multilevel inverters controlled by Pulse Wide Modulation (PWM) are being increasingly preferred for high-power applications [6] such as wind power generation. The multilevel topology not only increases the power rating, but also reduces stress across the switches and improves the voltage waveforms with lower harmonic content.

This paper presents an ideal combination of the modulation strategy known as Pulse Wide Modulation (PWM) applied to a three phase NPC three-level inverter in order to optimize the power output. The proposed technique controls active and reactive powers of the wind turbine based on the DFIG via the control of rotor currents.

This article discus about the control of stator active and reactive powers of the DFIG connected directly to the grid by the stator side and fed by an NPC three level PWM technique using different controllers PI, ANNPI and ANN.

## 2 Modelling of the wind turbine

The aerodynamic power  $P_{tur}$  captured by the wind turbine is given by [12–22]:

$$P_{tur} = 12C_p(\lambda, \beta) \rho S v^3, \quad (1)$$

where:  $\rho$  is the air density (1.25 kg/m<sup>3</sup>);  $S$  is wind turbine blades swept area in the wind (m<sup>2</sup>);  $R$  is the turbine

radius (m);  $V$  is wind speed (m/s);  $\beta$  blade pitch angle (°) and  $\lambda$  is the tip-speed ratio defined by:

$$\lambda = \frac{\Omega_{tur} R}{v}. \quad (2)$$

$C_p$  is the power coefficient of wind is treated in bibliographies for a wind of 4 KW [7, 8] by:

$$C_p(\lambda, \beta) = (0.5 - 0.0167(\beta - 2)) \sin \left[ \frac{\pi \cdot (\lambda + 0.1)}{10 - 0.3 \cdot \beta} \right] - 0.00184 \cdot (\lambda - 3) \cdot (\beta - 2). \quad (3)$$

The characteristics of the wind will determine the amount of energy that can be extracted from the wind farm actually [6]. The wind speed will be modelled in deterministic form by a sum of several harmonics:

$$V_v = 8 + 0.2 \sin(0.1047 t) + 2 \sin(0.2665 t) + 0.2 \sin(3.6645 t). \quad (4)$$

Expression of the aerodynamic torque is given by [7]:

$$T_{tur} = P_{tur} \Omega_{tur} = \frac{\pi}{2\lambda} \rho R^3 C_p(\lambda, \beta). \quad (5)$$

The gearbox is the connection between the turbine and the generator modelled by [17]:

$$T_{mec} = T_{tur} G, \quad (6)$$

$$\Omega_{mec} = G \Omega_{tur}, \quad (7)$$

where:  $T_{mec}$  is mechanical torque,  $\Omega_{tur}$ ,  $\Omega_{mec}$  are the turbine and generator speed, and  $G$  is the gearbox ratio.

The equation of system dynamics, can be written as [17]:

$$J \frac{d\Omega_{mec}}{dt} + f \Omega_{mec} = T_{mec} - T_{em}, \quad (8)$$

where:  $f$  is the viscous friction coefficient,  $T_{em}$  is the electromagnetic torque of the generator.  $C_p(\lambda, \beta)$  illustrated in Fig. 1, in our case  $C_{p,opt} = 0.48$  is obtained for  $\beta = 0$  and  $\lambda = \lambda_{opt} = 8$ .

## 3 Modelling of Doubly Fed Induction Generator

We present in preferred way the dynamics electrical model of the DFIG-generator in a synchronous reference frame ( $d, q$ ) rotating at an angular speed of  $\omega_s$ . According to [14–23], the basic equations used to model the DFIG-generators in the rotating d–q reference frame are written as [24–26]:

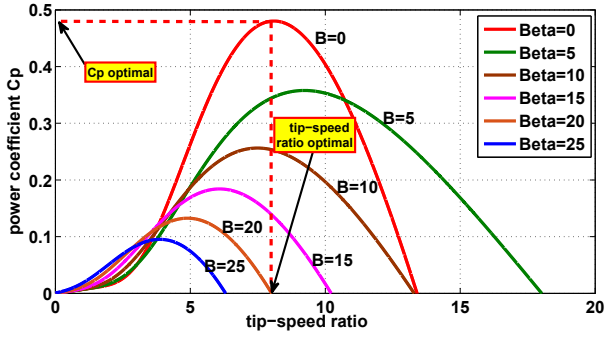


Fig. 1 Power coefficient variation against  $\lambda$  and  $\beta$

$$\begin{cases} V_{sd} = R_s I_{sd} + \frac{d\varphi_{sd}}{dt} - \omega_s \varphi_{sq} \\ V_{sq} = R_s I_{sq} + \frac{d\varphi_{sq}}{dt} + \omega_s \varphi_{sd} \\ V_{rd} = R_r I_{rd} + \frac{d\varphi_{rd}}{dt} - (\omega_s - \omega_r) \varphi_{rq} \\ V_{rq} = R_r I_{rq} + \frac{d\varphi_{rq}}{dt} + (\omega_s - \omega_r) \varphi_{rd} \end{cases} \quad (9)$$

The stator and rotor flux are expressed by [4, 5]:

$$\begin{cases} \varphi_{sd} = L_s I_{sd} + M I_{rd} \\ \varphi_{sq} = L_s I_{sq} + M I_{rq} \\ \varphi_{rd} = L_r I_{rd} + M I_{sd} \\ \varphi_{rq} = L_r I_{rq} + M I_{sq} \end{cases} \quad (10)$$

where:  $R_s, R_r, L_s$  and  $L_r$  are respectively the resistance and inductance of the stator and the rotor;  $M$  is the mutual inductance,  $I_{sd}, I_{sq}, I_{rd}, I_{rq}$  represent the  $d$  and  $q$  components of the stator and rotor currents;  $\omega_s$  is the stator angular frequency ( $\omega_r = \omega_s - P\Omega_{mec}$ );  $\omega_r$  is rotor angular frequency, and  $P$  number of pole pairs.

Equation (11) represents the expression of electromagnetic torque [2, 9, 26–28]:

$$T_{em} = P \frac{M}{L_s} (\varphi_{sd} I_{rq} - \varphi_{sq} I_{sd}) \quad (11)$$

Expression of active and reactive power:

$$\begin{cases} P_s = V_{sd} I_{sd} + V_{sq} I_{sq} \\ Q_s = V_{sq} I_{sq} - V_{sd} I_{sd} \end{cases} \quad (12)$$

$$\begin{cases} P_r = V_{rd} I_{rd} + V_{rq} I_{rq} \\ Q_r = V_{rq} I_{rq} - V_{rd} I_{rd} \end{cases} \quad (13)$$

#### 4 Field Oriented Strategy (FOC)

In Section 4, we proposed a vector control law for DFIG machine based on the orientation of the stator flux. It is a natural decoupling between the magnitude controlling the flux (the excitation current) and that related to the torque (the armature current). This decoupling provides a very fast torque response, a large speed control range and high efficiency for a large steady state load range [22].

Examination of the expression of the torque of the machine shows that it results from a difference between two quadrature components of the stator current and rotor flux which has a complex coupling between the machine magnitudes. The working reference for the control is that related to the rotating field so that the axis ( $d$ ) coincides with the direction desired flow, which can be rotor, stator, or air gap. Thus, it is possible to orient the different flows of the machine [3, 17–29].

The stator flux with the conditions:

$$\begin{cases} \varphi = \varphi_{sd} = \varphi_s \\ \varphi_{sq} = 0 \end{cases} \quad (14)$$

The rotor flow with the conditions:

$$\begin{cases} \varphi = \varphi_{rd} = \varphi_r \\ \varphi_{rq} = 0 \end{cases} \quad (15)$$

Starting from Eq. (11), a decoupling can be performed in such a way that the torque will be controlled solely by the current  $I_{rq}$  and thus the flow by the current  $I_{rd}$ . The final relationship of the couple is:

$$T_{em} = P \frac{M}{L_s} (\varphi_{sd} I_{rq}) \quad (16)$$

$$\begin{cases} V_{sd} = 0 \\ V_{sq} = V_s = \omega_s \varphi_s \end{cases} \quad (17)$$

$$\begin{cases} \varphi_{sd} = L_s I_{sd} + M I_{rd} \\ 0 = L_s I_{sq} + M I_{rq} \end{cases} \quad (18)$$

The rotor voltages are given by flowing expression:

$$V_{rd} = R_r I_{rd} + L_r \sigma \frac{dI_{rd}}{dt} - g \omega_s L_r \sigma I_{rq} \quad (19)$$

$$V_{rq} = R_r I_{rq} + L_r \sigma \frac{dI_{rq}}{dt} + g \frac{M}{L_s} V_s + g \omega_s L_r \sigma I_{rd} \quad (20)$$

We get the following expressions for the active and reactive powers [27]:

$$\begin{cases} P_s = -V_s \frac{M}{L_s} I_{rq} \\ Q_s = \frac{V_s \varphi_s}{L_s} + \frac{V_s M}{L_s} I_{rd} \end{cases} \quad (21)$$

It can be noticed that active power and reactive powers are independently controlled respectively by quadrature and direct rotor currents. Thus, it is easy to answer new grid codes requirements in term of  $PQ$  profiles.

According to Eq. (21) active and reactive powers can be controlled via rotor currents. That is why we call this approach indirect method [25–29].

The currents references are deduced as follow:

$$I_{rqref} = \left( -\frac{L_s}{V_s M} \right) P_s, \quad (22)$$

$$I_{rdref} = \left( Q_s - \frac{L_s}{V_s \varphi_s} \right) \frac{L_s}{V_s M}. \quad (23)$$

The PI controller expression is:

$$F(p) = K_i + \frac{K_p}{p}. \quad (24)$$

With poles compensation approach, proportional and integral gains are expressed as follow:

$$K_{p1} = \frac{3\sigma L_r}{T_r}, \quad (25)$$

$$K_{i2} = \frac{3R_r}{T_r}, \quad (26)$$

where  $T_r = 3\tau = \frac{3\sigma L_r}{K_p}$  is response time at 95% that we fix according to the global dynamic requested for the system. The active and reactive powers can be controlled by the using of direct method [28]. The active and reactive powers become:

$$P_s = \frac{-V_s \frac{M}{L_s}}{R_r + \sigma L_r p} V_{rq}, \quad (27)$$

$$Q_s = \frac{V_s \varphi_s}{L_s} + \frac{\frac{V_s M}{L_s}}{R_r + \sigma L_r p} V_{rd}. \quad (28)$$

With poles compensation approach, proportional and integral gains are expressed as follow:

$$K_{p3} = \frac{-3L_r L_s}{T_r M V_s}, \quad (29)$$

$$K_{i4} = \frac{3R_r L_s}{T_r M V_s}. \quad (30)$$

### 5 NPC three level inverter

An NPC three-phase three-level converter is shown in Fig. 2. The three phases have a common  $dc$  bus, divided

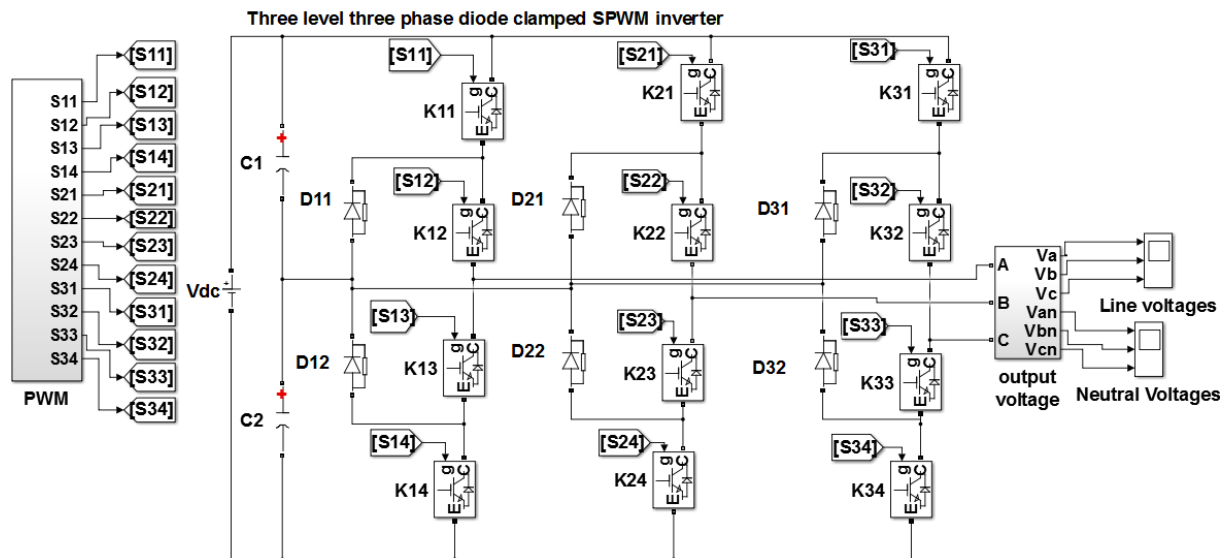


Fig. 2 NPC three-level inverter structure

by two capacitors into three levels. The voltage across each capacitor is  $\frac{V_{dc}}{2}$ ; and the voltage stress across each switching device is limited to  $\frac{V_{dc}}{2}$  through the clamping diodes. A three-level NPC converter can able to produce five levels of line-to-line voltage and three levels of phase voltage. This NPC converter reduces harmonics in both voltage and current output [6–16].

Table 1 gives the switch states for phase a similar switching sequence will be derived for other phases by according the phase angle displacement. Here, K11 and K13 are complement of each other and K12 and K14 are complement of each other [19].

### 6 NPC pulse width modulation strategy

An NPC inverter includes the DC power source to output DC voltage having a neutral point. An NPC convert DC voltage into AC voltage in three phases PWM control. When a mode is selected, consider to a first and a second PWM modes by comparing amplitude of voltage reference with a predefined value that is defined by a minimum pulse width, a first voltage reference means to add a predefined bias value at which a changes to positive/negative within a fixed period to voltage references in respective phases in a first PWM mode, a second voltage reference means to fix the voltage reference in one phase by a value with minimum pulse width when voltage reference in one phase is smaller than a described value that is defined by the minimum pulse width in a next PWM mode and correct voltage references of other two phases so as to make line voltage to a value corresponding to the voltage reference, and a modulation frequency varied over to lower PWM control modulation frequency in the first PWM mode and to suppress power loss caused by switching in the first PWM mode [10].

Fig. 3 shows modulation strategy for NPC three levels inverter. PWM strategy is applied for arms. In Fig. 3, C1 and C2 are triangular carriers of three arm (a, b, c), Va represents modulation wave of arm A. The phase of C1

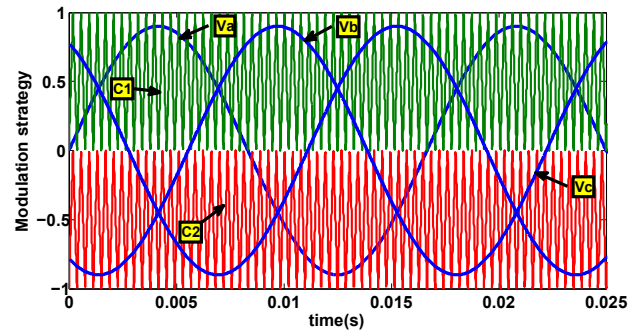


Fig. 3 Modulation strategy of NPC three-levels inverter

is opposite with C2. When the value of Va is higher than C1, K11 and K12 are switched on. When the value of Va is lower than C2, K13 and K14 are switched on. In the other case, K12 and K13 are turned on, and the output level is 0. Similarly, C1 and C2 are triangular carriers of arms B and C, Vb represents modulation wave of arm B and Vc represents modulation wave of arm C. Same principle applied for arm a is applied for two arms B and C.

In Fig. 4 and Fig. 5 we can clearly observed the three level for one output phase and one output line generated by the NPC inverter. In Fig. 4 the positive voltage levels corresponds to  $0, \frac{V_{dc}}{2}, V_{dc}$ , all totaling, while the negative output voltage level corresponds to  $0, -\frac{V_{dc}}{2}, -V_{dc}$ , all totaling, all totaling to a three levels.

Fig. 6 shows the model scheme of the vector control of DFIG. The power control strategy is presented on Fig. 6, where PI regulators are used for current loops, as well as for power loops.

### 7 Artificial Neural Network control

The Artificial Neural Networks are generally designed to solve real problems encountered in different branches of engineering. ANN is usually optimized by different learning methods, and can be used for statistical applications, or as an artificial intelligence method to which

**Table 1** switch states for NPC tree level inverter

| States of switches |     |     |     | Voltages level      |
|--------------------|-----|-----|-----|---------------------|
| K11                | K12 | K13 | K14 |                     |
| 1                  | 1   | 0   | 0   | $\frac{V_{dc}}{2}$  |
| 0                  | 1   | 1   | 0   | 0                   |
| 0                  | 0   | 1   | 1   | $-\frac{V_{dc}}{2}$ |
| 0                  | 0   | 1   | 0   | 0                   |

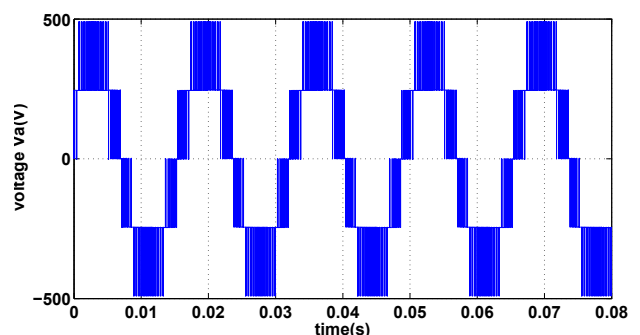


Fig. 4 Output voltage phase of NPC three levels inverter

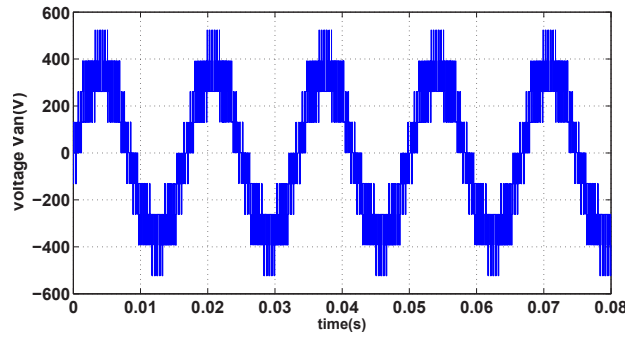


Fig. 5 Output voltage line of NPC three levels inverter

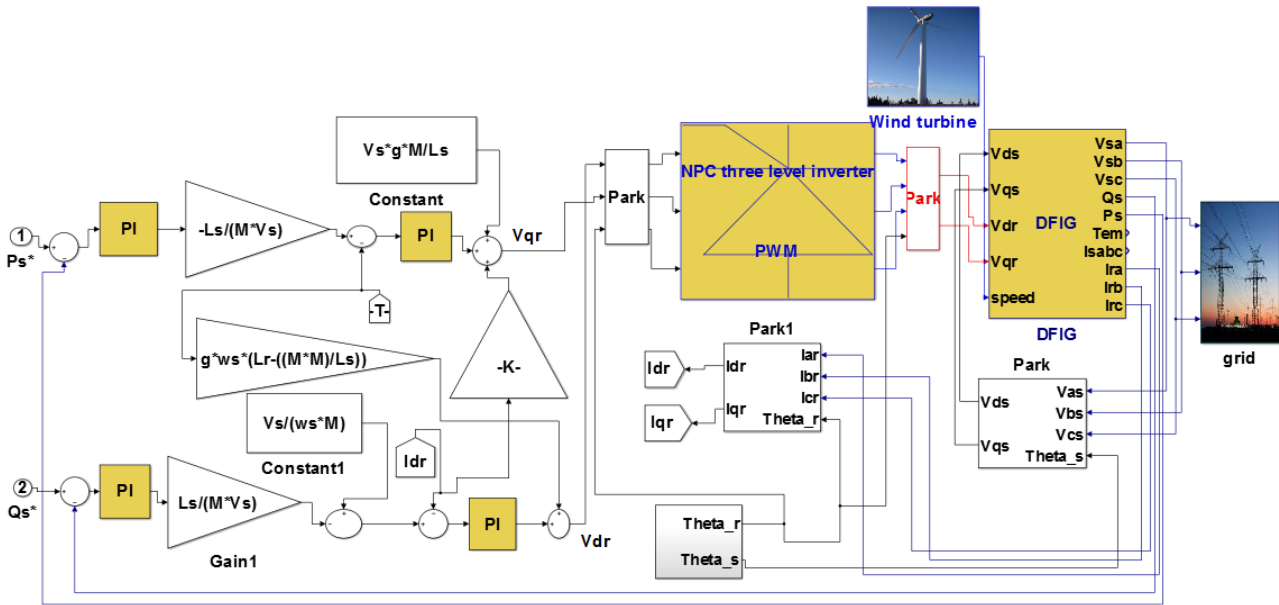


Fig. 6 Block diagram of the field oriented control of DFIG

they provide a perceptual mechanism. Recently, in the field of electrical control, ANN has been used for their learning ability, fast processing and accuracy. The general feed forward structure shown in Fig. 7, consists of

three layers, input-output, and hidden layers with  $n$ ,  $k$ , and  $m$  neurons, respectively. The signal propagation of each layer is described in detail as follows:

The signal propagation of each layer is described in detail as follows:

$$U_j = X(j), \text{ with } j = 1, 2, 3, \dots, n, \quad (31)$$

where,  $U_j$  denotes the  $j^{\text{th}}$  neuron used for the input layer, and the  $n$  neurons number depend on the process complexity.

The input and output on the hidden layer are:

$$v_i = \sum_{j=1}^n U_j w_{ij}, \quad (32)$$

$$y_i = f(v_i) = f\left(\sum_{j=1}^n U_j w_{ij}\right), \text{ with } i = 1, 2, 3, \dots, m, \quad (33)$$

where  $y_i$  is the total input of  $i^{\text{th}}$  neuron used for the hidden layer,  $w_{ij}$  is the weight values, and  $f(*)$  denotes the activation function.

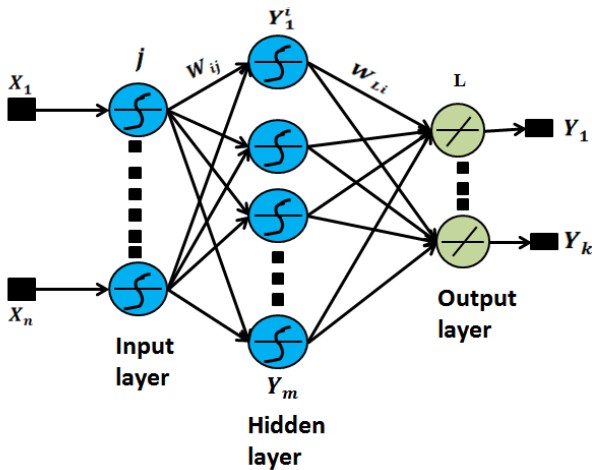


Fig. 7 Configuration of ANN control

The input of the output layer is:

$$Z_L = \sum_{L=1}^k y_i w_{Li} = \sum_{L=1}^k f(v_i) w_{Li}. \quad (34)$$

The total output of the neural network can be represented by Eq. (35):

$$y_k = f(Z_L) = f\left(\sum_{L=1}^k f(v_i) w_{Li}\right) = f\left(\sum_{L=1}^k w_{Li} f\left(\sum_{j=1}^n U_j w_{ij}\right)\right). \quad (35)$$

### 8 Active reactive powers Artificial Neural Network Proportional Integral Control

The Artificial Neural Network (ANN) is widely used in many fields of technology application and scientific re-search. This technique can be used in cases of difficult problems that cannot be described by precise mathematical approaches where they are very complicated to manipulate [18, 20, 24]

This method was proposed to improve the quality of the current and power generated by the generator-based wind turbine system. The proposed FOC technique is simple to control and easy to implement. Also, the combination between this proposed FOC and intelligent control, the dynamic response of the generator is greatly improved. This proposed method is a change in the form of the classical method, where neural networks are used with combination with the conventional PI controller [3–17].

In this work, the weight and bias of the neural network are selected based on the use of a Levenberg-Marquardt

algorithm. This is by using the word trainlm (the network training function) in the Matlab software. However, the Levenberg-Marquardt technique is a robust algorithm and quick technique compared to other methods.

The main idea of this control is to use two Artificial Neural Networks based controllers to control stator active and reactive powers independently combined with two classic controllers PI for active and reactive power. Fig. 8 shows the model scheme of DFIG active and reactive powers control using ANN controllers combined with PI controllers (ANNPI controller). Fig. 9 shows the diagram of ANNPI numerical controller, that the two Artificial Neural Networks are a Multilayer Perceptron networks (MLP) with a structure of (2-5-1). The first ANN inputs are the measured and reference stator active power, and the output is the input of stator power PI controller. Inputs of the second ANN are the measured and reference stator reactive power, and the output is the input of second stator reactive power PI controller.

Compared with the classical FOC method used stator active and reactive power PI controller, the Artificial Neural Network Proportional Integral (ANNPI) method ensures diverse advantages such as the reduction of active power ripples, torque ripples, and reactive power ripples.

Fig. 9 shows the architecture of Neural Network, it is a network with two layers: layer1 is the hidden layer and layer 2 is output layer.

The convergence of the network in summer obtained by using the value of the parameters grouped in Table 2.

Fig. 10 shows the training performance plot for DFIG active and reactive powers control ANN which is combined

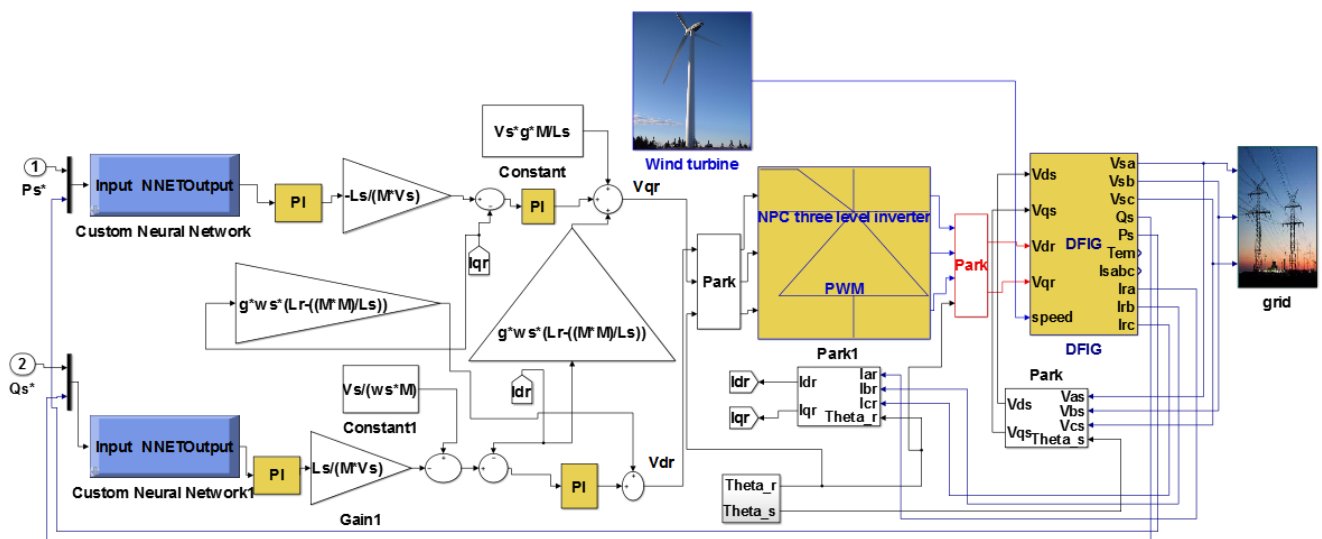


Fig. 8 Block diagram of the ANNPI active and reactive power controller of DFIG

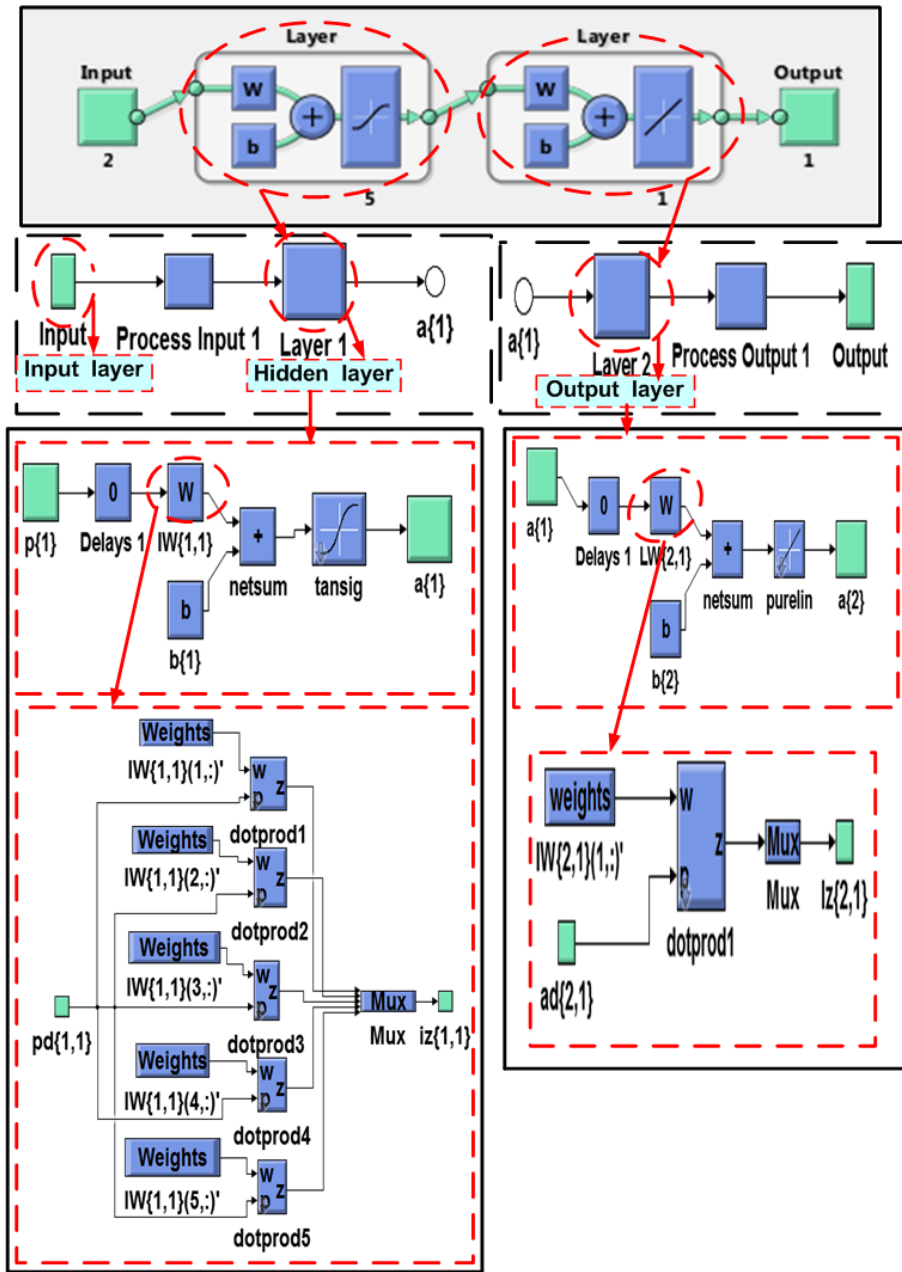


Fig. 9 Block diagram of numerical controller: Input layer; Hidden layer; Output layer

Table 2 Parameters of the LM for switching controller

| Parameters of the LM    | Values                   |
|-------------------------|--------------------------|
| Number of hidden layer  | 5                        |
| TrainParam.Lr           | 0.02                     |
| TrainParam.show         | 50                       |
| TrainParam.eposh        | 3000                     |
| TrainParam.goal         | 1e-30                    |
| Functions of activation | Tansig, Purling, Trainlm |

with PI controller. Training performance is based on mean square error between desired output and actual output of ANN.

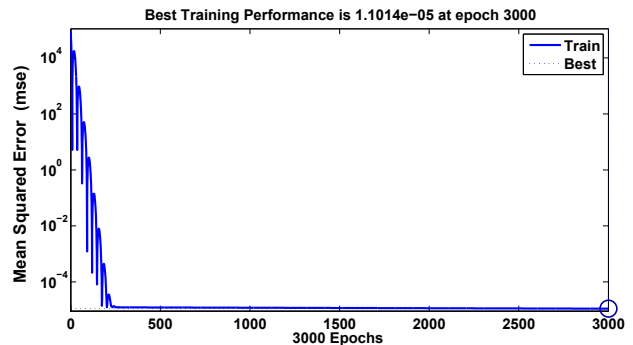


Fig. 10 Training performance for DFIG active and reactive powers control ANN

### 9 Active reactive powers Artificial Neural Network Control

The main idea of this control is to replace PI stator active and reactive power controller by two Artificial Neural Networks based controllers to control stator active and reactive powers independently. Fig. 11 shows the ANN controller of stator active and reactive power of DFIG associated NPC three levels inverter [4, 13, 20].

In neural networks, output and input layer neurons are selected according to the number of inputs and outputs of the system, respectively. The number of entries is one in the entry layer, so the number of cells is only one. As for the output layer, there is only one output, so there is only one cell. We chose only one hidden layer and 12 neurons in the hidden layer [15, 17, 21].

Fig. 12 presented the Block diagram of ANN numerical controller, two Artificial Neural Networks are a Multilayer Perceptron networks (MLP) with a structure of (1-12-1). The first ANN inputs are the error stator active power, and the output is the Park quadratic current reference  $I_{rq}$ . Inputs of the second ANN is error stator reactive power, and the output is the Park direct reference current  $I_{rd}$ . The active and reactive powers are independently controlled. Stator active power ( $P_s$ ) is controlled via rotor Park quadratic current ( $I_{rqref}$ ), while stator reactive power ( $Q_s$ ) is controlled via rotor Park direct current ( $I_{rdref}$ ).

The convergence of the network in summer obtained by using the value of the parameters grouped in Table 3. The main parameters of the wind turbine are given in Table 4

in the Appendix and the main parameters of the DFIG are given in Table 5 in the Appendix. Fig. 13 shows the training performance plot for DFIG active and reactive powers control ANN that replace PI controller. Training performance is based on mean square error between desired output and actual output of ANN.

### 10 Results and discussion

The simulation study has been carried out using MATLAB environment. The simulation results show the application of field-oriented control with NPC three levels inverter of the DFIG shows the use of different stator active and reactive controllers (PI, ANNPI, ANN). Both control techniques PI, ANNPI, ANN are simulated and compared in terms of reference tracking, powers ripples and performance.

Fig. 14 shows the stator active power response of DFIG due to change in reference stator active power, the stator active power track almost perfectly their references values. Moreover, the results of simulations have shown that the application of ANNPI control gives a good response of active power and power level ripples are lower compared to conventional PI controller, so the combination of ANN with PI improved classical controller response.

According to the simulation results shown in Fig. 14, the ANN controller we show that the amplitudes of the ripples of the stator active power are smaller and occur in a shorter period in comparison with the ripples obtained for the ANNPI command and PI command. The proposed ANN control ensures the best optimal power tracking

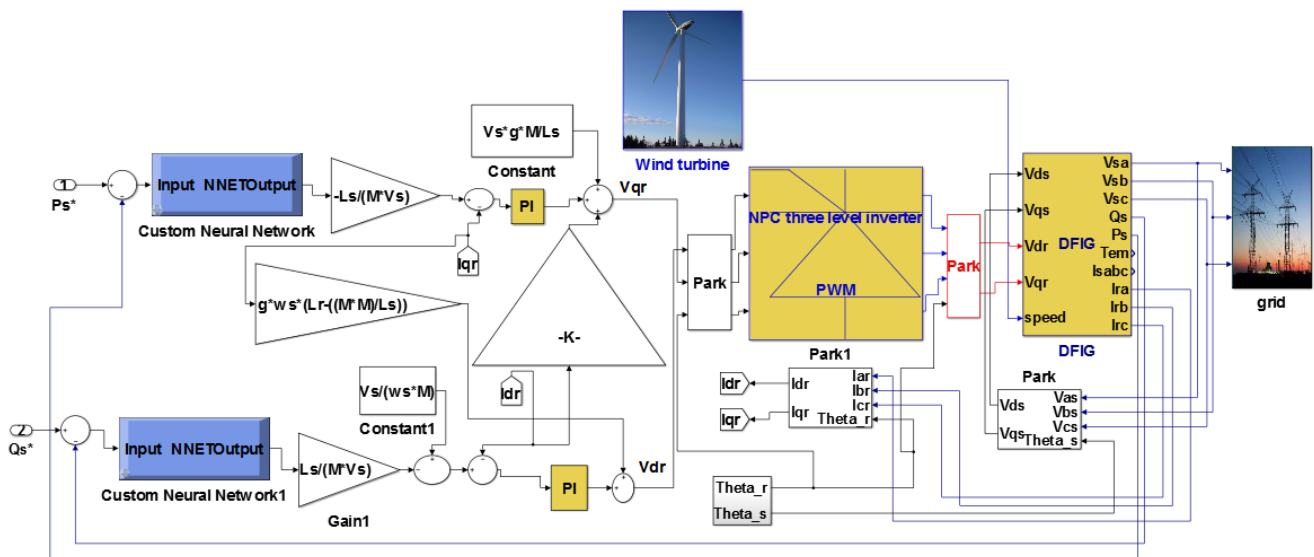


Fig. 11 Block diagram of the ANN active and reactive powercontroller of DFIG

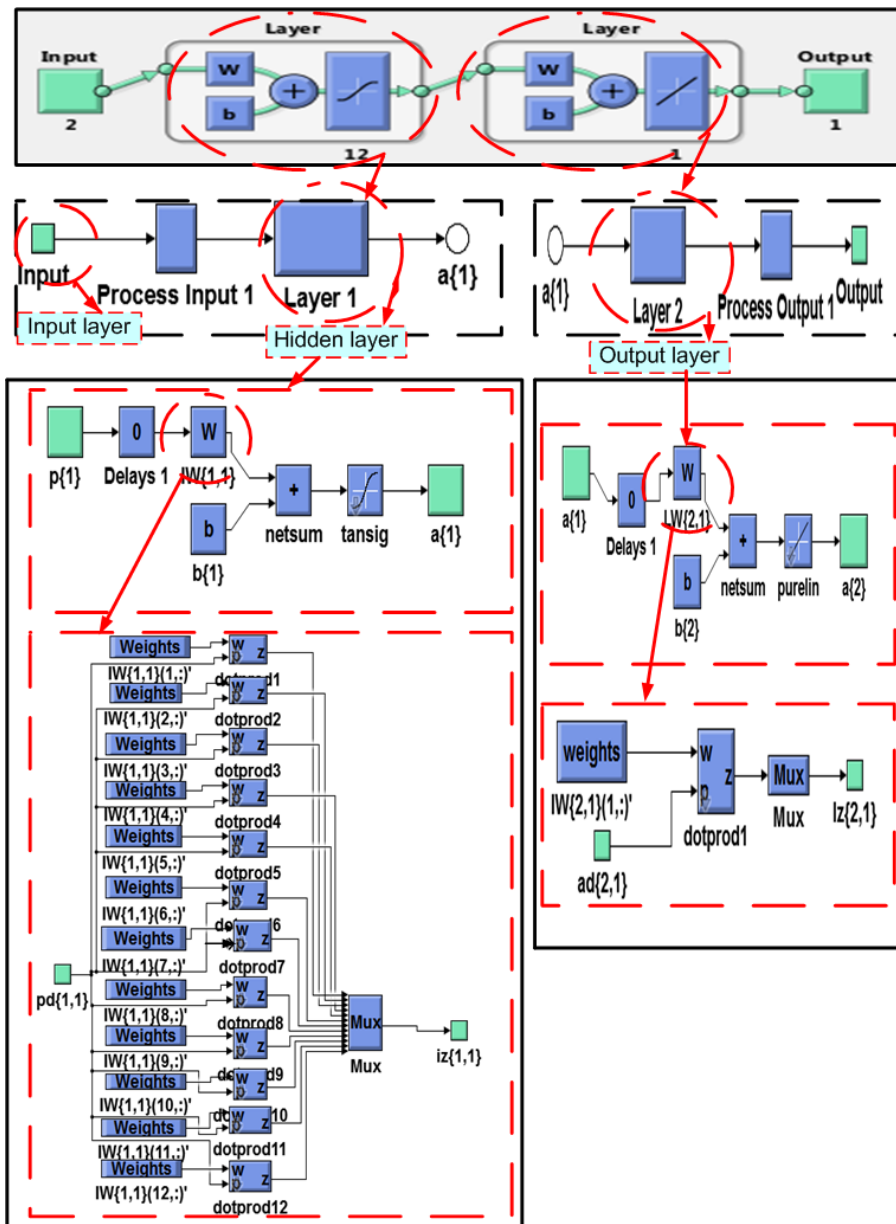


Fig. 12 The internal structure of proposed ANN controller: Input Layer; Hidden Layer; Output Layer

Table 3 Parameters of the LM for switching controller

| Parameters of the LM    | Values                   |
|-------------------------|--------------------------|
| Number of hidden layer  | 12                       |
| TrainParam.Lr           | 0.02                     |
| TrainParam.show         | 50                       |
| TrainParam.eposh        | 3000                     |
| TrainParam.goal         | 1e-40                    |
| Functions of activation | Tansig, Purling, Trainlm |

performance and the reduction of ripple of stator active power compared with the classical PI and ANNPI control.

Fig. 15 shows the obtained simulation results PI, ANNPI and ANN control stator reactive power, tracks

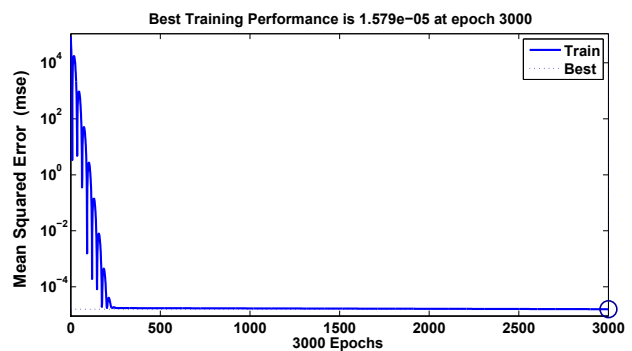


Fig. 13 Training performance for DFIG active and reactive powers control ANNs

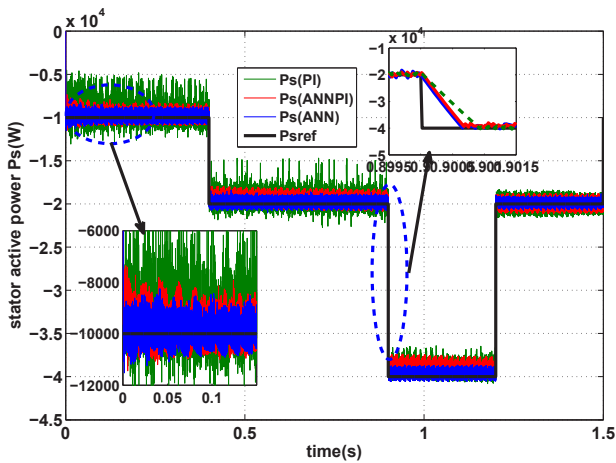


Fig. 14 Stator active power (PI, ANNPI, ANN)

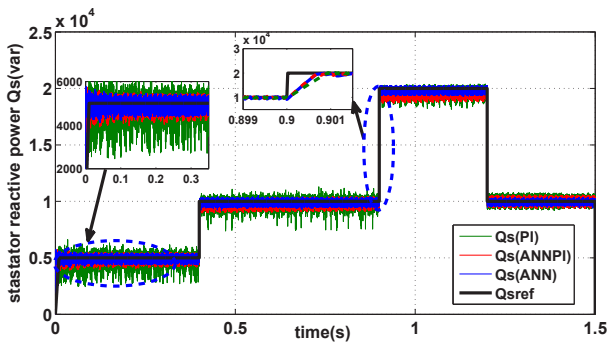


Fig. 15 Stator reactive power (PI, ANNPI, ANN)

almost perfectly their references values. Moreover, the ANNPI control minimized the stator reactive power ripple compared to the PI controller.

The simulation result obtained by ANN controller show good performances in following the reactive power. When the reference when changes, it is noticed that the oscillations decrease.

The simulation results obtained leads us to conclude that the neural network controller is a good following to

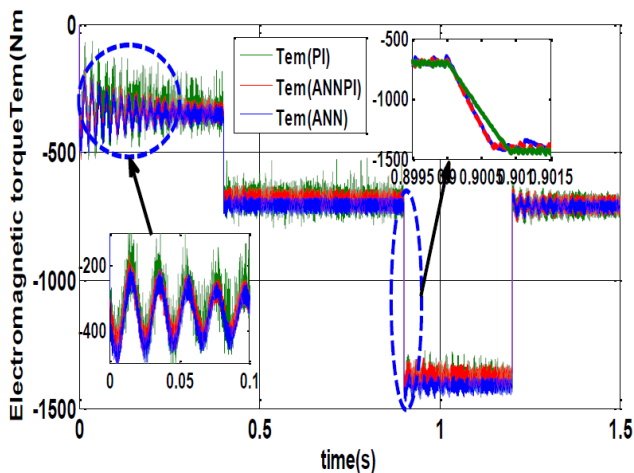


Fig. 16 Electromagnetic torque (PI, ANNPI, ANN)

reference, and it does not present oscillation compared to ANNPI and PI controllers.

Fig. 16 shows the waveforms of the torque. It can be said by comparing Fig. 14 with Fig. 12 the value of the torque is related to the value of the active power. On the other hand, the proposed technique ANN reduced the torque ripples compared to the ANNPI and PI technique. It is shown that the ANN controller has high effectiveness compared to the traditional PI and ANNPI controller.

The currents generated by the wind turbine Doubly Fed Induction Generator system with the PI, ANNPI and ANN strategies are shown in Fig. 17(a), (b) and (c). The passage between operating modes is zoomed in these figures indicating 50 Hz frequency. One can clearly see that the ANN

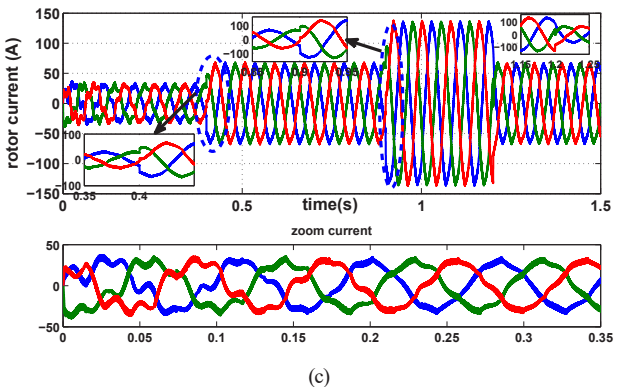
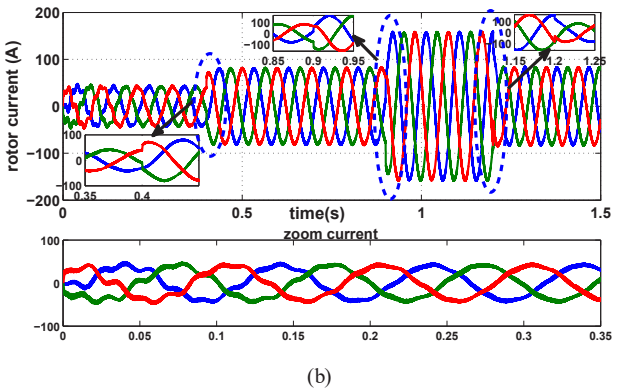
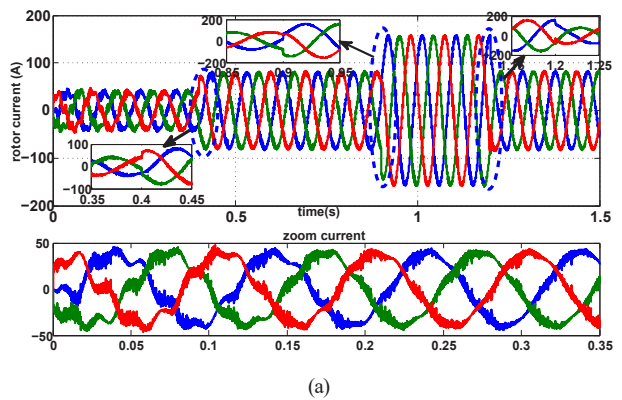


Fig. 17 Rotor current and their zoom; (a) PI; (b) ANNPI; (c) ANN

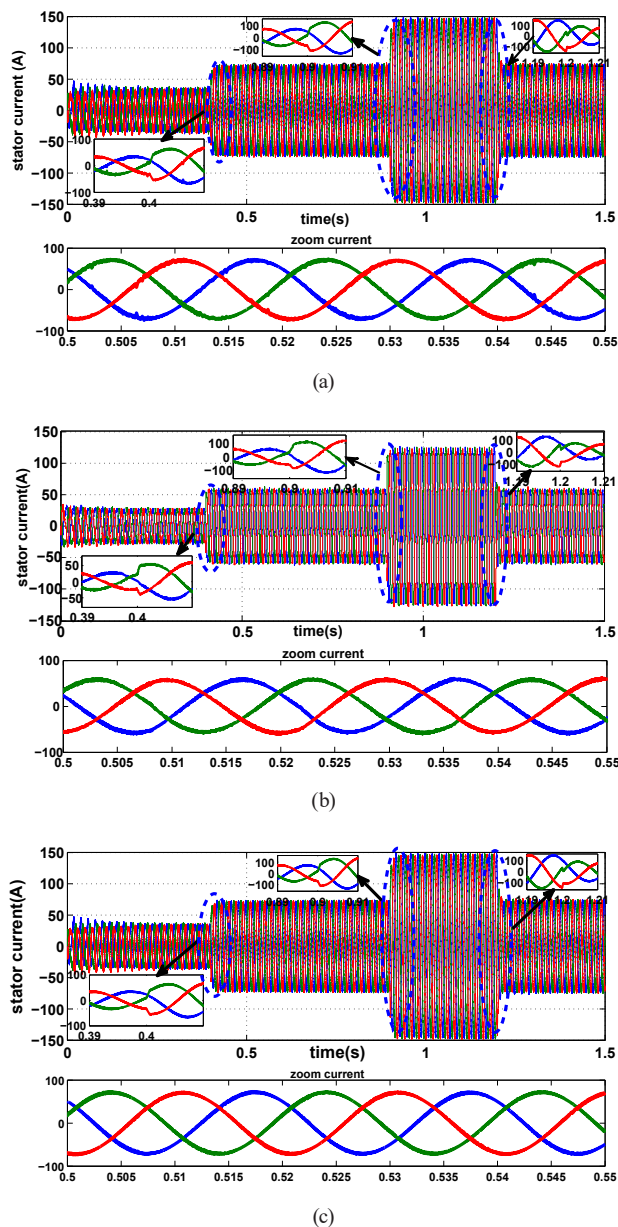


Fig. 18 Stator current and their zoom; (a) PI; (b) ANNPI; (c) ANN

and ANNPI proposed controllers' technique significantly improve the current quality compared to the one obtained with PI. We can observe in zoom Fig. 17(a), (b) and (c) that the phase rotor currents have almost sinusoidal shapes in transient regime given by ANN and ANNPI controller compared to PI controller.

Fig. 18(a), (b) and (c) show the stator currents generated by the wind turbine Doubly Fed Induction Generator system with the PI, ANNPI and ANN controllers and the passage between operating modes which are zoomed in this figures indicating 50 Hz frequency.

The results obtained from zoom stator current Fig. 18(a), (b) and (c) show that for the proposed controller ANN and

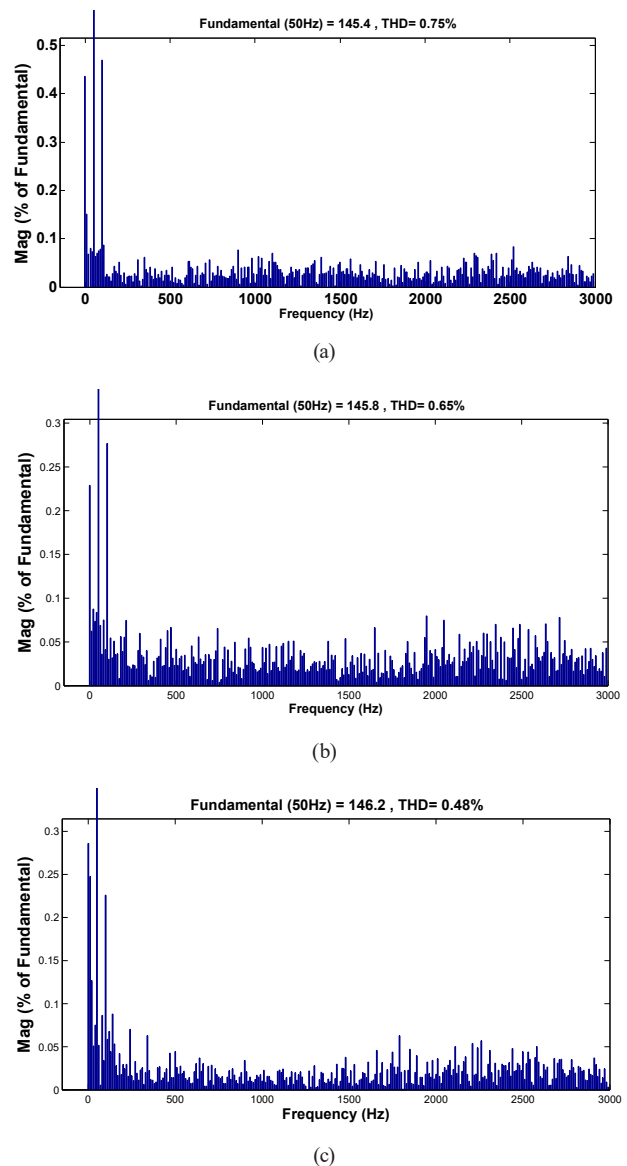


Fig. 19 Spectrum harmonic of one phase stator current for (a) PI; (b) ANNPI; (c) ANN

ANNPI the phase stator currents have almost sinusoidal shapes, which means that a good quality energy is supplied to the network.

Fig. 19(a), (b) and (c) shows the harmonic spectrum of one phase stator current of the DFIG obtained using Fast Fourier Transform (FFT) technique for the three controllers. It can be clear observed that the total harmonic distortion (THD) is reduced for ANNPI (THD = 0.65%) compared PI controller (THD = 0.75%). It can be clearly observed through these parts of Fig. 19 that the THD value is more reduced for the ANN (THD = 0.48%) compared PI and ANNPI controller.

Therefore it can be concluded that the proposed controller (ANN) has proven effective in reducing the value of the total harmonic distortion.

## 11 Conclusion

The vector control scheme of a DFIG connected directly to the grid by the stator side and fed by an NPC three level PWM technique to reduce the total harmonic disturbance has been presented in this work.

The aim of this paper is to study a system which converts wind energy into electrical energy. In this paper, we represented the vector control with application of classical PI, ANNPI and ANN controller, are used to control the stator active and reactive power of the DFIG injected in the grid. Simulation studies are conducted to verify the performance of the proposed PI controller. The proposed controller does not provide high-performance dynamic characteristic and give more and more ripple in different response. The combination of classical PI control and intelligent (ANNPI) controller shown the good

performance of this proposed control, regarding reference tracking and power ripples reduction. The generated currents kept sinusoidal form with a constant frequency. An FFT analysis of the generated current indicated a significant reduction of total harmonic distortion currents during all operations and compensation modes.

With the ANN controller is synthesized and compared to traditional PI and ANNPI controllers. The simulation results show that with ANN controller is an excellent solution for DFIG based wind turbines in terms of tracking performances reactive and active powers references, and THD of the stator current. Furthermore, the obtained results have approved that with ANN controller minimizes the THD value of the stator current, and powers ripples more and more reduced than the classical PI and ANNPI controllers.

## References

- [1] Bounadja, E., Djahbar, A., Boudjema, Z. "Variable Structure Control of a Doubly Fed Induction Generator for Wind Energy Conversion Systems", *Energy Procedia*, 50, pp. 999–1007, 2014. <https://doi.org/10.1016/j.egypro.2014.06.119>
- [2] Yaichi, I., Semmah, A., Wira, P. "Direct Power Control of Wind Turbine Based on Doubly Fed Induction Generator", *European Journal of Electrical Engineering*, 21(5), pp. 457–464, 2019. <https://doi.org/10.18280/ejee.210508>
- [3] Boubzizi, S., Abid, H., El hajjaji, A., Chaabane, M. "Comparative study of three types of controllers for DFIG in wind energy conversion system", *Protection and Control of Modern Power Systems*, 3(1), Article number: 21, 2018. <https://doi.org/10.1186/s41601-018-0096-y>
- [4] Sahri, Y., Tamalouzt, S., Hamoudi, F., Belaid, S. L., Bajaj, M., Alharthi, M. M., Alzaidi, M. S., Ghoneim, S. S. M. "New intelligent direct power control of DFIG-based wind conversion system by using machine learning under variations of all operating and compensation modes", *Energy Reports*, 7, pp. 6394–6412, 2021. <https://doi.org/10.1016/j.egypr.2021.09.075>
- [5] Kaloi, G. S., Wang, J., Baloch, M. H. "Active and reactive power control of the doubly fed induction generator based on wind energy conversion system", *Energy Reports*, 2, pp. 194–200, 2016. <https://doi.org/10.1016/j.egypr.2016.08.001>
- [6] Benboughenni, H., Boudjema, Z., Belaidi, A. "Power Control of DFIG in WECS Using DPC and NDPC-NPWM Methods", *Mathematical Modelling of Engineering Problems*, 7(2), pp. 223–236, 2020. <https://doi.org/10.18280/mmep.070208>
- [7] Taleb, M., Cherkaoui, M. "Active and Reactive Power Control of Doubly Fed Induction Generator Wind Turbines to Answer Grid Codes Requirements", *Journal of Clean Energy Technologies*, 6(2), pp. 101–105, 2018. <https://doi.org/10.18178/jocet.2018.6.2.442>
- [8] Zerzouri, N., Labar, H. "Active and Reactive Power Control of a Doubly Fed Induction Generator", *International Journal of Power Electronics and Drive Systems (IJPEDS)*, 5(2), pp. 244–251, 2014. <https://doi.org/10.11591/ijpeds.v5i2.6477>
- [9] Senani, F., Rahab, A., Benalla, H. "A Complete Modeling and Control for Wind Turbine Based of a Doubly Fed Induction Generator using Direct Power Control", *International Journal of Power Electronics and Drive Systems (IJPEDS)*, 8(4), pp. 1954–1962, 2017. <https://doi.org/10.11591/ijpeds.v8.i4.pp1954-1962>
- [10] Hachemi, H., Allali, A., Belkacem, B. "Control of the power quality for a DFIG powered by multilevel inverters", *International Journal of Electrical and Computer Engineering (IJECE)*, 10(5), pp. 4592–4603, 2020. <https://doi.org/10.11591/ijece.v10i5.pp4592-4603>
- [11] Moualdia, A., Mahoudi, M. O., Nezli, L., Bouchhida, O. "Modelling and Control of a Wind Power Conversion System Based on the Double-fed Asynchronous Generator", *International Journal of Renewable Energy Research*, 2(2), pp. 300–306, 2012. <https://doi.org/10.20508/ijrer.v2i2.193.g118>
- [12] Louarem, S. L. S., Belkhiat, D. E. C., Bouktir, T., Belkhiat, S. "An Efficient Active and Reactive Power Control of DFIG for a Wind Power Generator", *Engineering, Technology & Applied Science Research*, 9(5), pp. 4775–4782, 2019. <https://doi.org/10.48084/etasr.3007>
- [13] Mesai-ahmed, H., Bentaallah, A., Cardoso, A. J. M., Djeriri, Y., Jlassi, I. "Robust Neural Control of the Dual Star Induction Generator Used in a Grid-Connected Wind Energy Conversion System", *Mathematical Modelling of Engineering Problems*, 8(3), pp. 323–332, 2021. <https://doi.org/10.18280/mmep.080301>
- [14] Benboughenni, H., Bizon, N. "Advanced Direct Vector Control Method for Optimizing the Operation of a Double-Powered Induction Generator-Based Dual-Rotor Wind Turbine System", *Mathematics*, 9(19), Article number: 2403, 2021. <https://doi.org/10.3390/math9192403>
- [15] Benboughenni, H., Boudjema, Z., Belaidi, A. "Higher Control Scheme Using Neural Second Order Sliding Mode and ANFIS-SVM strategy for a DFIG-Based Wind Turbine", *International Journal of Advances in Telecommunications, Electrotechnics, Signals and Systems*, 8(2), pp. 17–28, 2019. <https://doi.org/10.11601/ijates.v8i2.263>

[16] Habib, B. "Robust Direct Power Control of a DFIG Fed by a Five-Level NPC Inverter Using Neural SVPWM Technique", *Tecnica Italiana-Italian Journal of Engineering Science*, 65(1), pp. 119–128, 2021.  
<https://doi.org/10.18280/ti-ijes.650118>

[17] Boudjellal, B., Benslimane, T. "Active and Reactive Powers Control of DFIG Based WECS Using PI Controller and Artificial Neural Network Based Controller", *Modelling, Measurement and Control A*, 93(1–4), pp. 31–38, 2020.  
[https://doi.org/10.18280/mmc\\_a.931-405](https://doi.org/10.18280/mmc_a.931-405)

[18] Tamaarat, A. "Active and Reactive Power Control for DFIG Using PI, Fuzzy Logic and Self-Tuning PI Fuzzy Controllers", *Advances in Modelling and Analysis C*, 74(2–4), pp. 95–102, 2019.  
[https://doi.org/10.18280/ama\\_c.742-408](https://doi.org/10.18280/ama_c.742-408)

[19] Tamalouzt, S., Belkhier, Y., Sahri, Y., Bajaj, M., Ullah, N., Chowdhury, M. S., Titseesang, T., Techato, K. "Enhanced Direct Reactive Power Control-Based Multi-Level Inverter for DFIG Wind System under Variable Speeds", *Sustainability*, 13(16), Article number: 9060, 2021.  
<https://doi.org/10.3390/su13169060>

[20] Jyothi, P., Prakash, R. B. R., Varma, P. S. "Application of Artificial Intelligence to DFIG based Wind Farm for Reactive Power Compensation", *International Journal of Renewable Energy Research*, 10(2), pp. 955–966, 2020.  
<https://doi.org/10.20508/ijrer.v10i2.10684.g7962>

[21] Zouheyr, D., Lotfi, B., Abdelmadjid, B. "Real-Time Emulation of a Grid-Connected Wind Energy Conversion System Based Double Fed Induction Generator Configuration under Random Operating Mode", *European Journal of Electrical Engineering*, 23(3), pp. 207–219, 2021.  
<https://doi.org/10.18280/ejee.230305>

[22] Moulay, F., Habbati, A., Hamdaoui, H. "Application and Control of a Doubly Fed Induction Machine Integrated in Wind Energy System", *Instrumentation Mesure Métrologie*, 18(3), pp. 257–265, 2019.  
<https://doi.org/10.18280/i2m.180305>

[23] Benakcha, M., Benalia, L., Ameer, F., Tourqui, D. E. "Control of dual stator induction generator integrated in wind energy conversion system", *Journal of Energy Systems*, 1(1), pp. 21–31, 2017.  
<https://doi.org/10.30521/jes.351269>

[24] Amer, M., Miloudi, A., Lakdja, F. "Optimal DTC Control Strategy of DFIG Using Variable Gain PI and Hysteresis Controllers Adjusted by PSO Algorithm", *Periodica Polytechnica Electrical Engineering and Computer Science*, 64(1), pp. 74–86, 2020.  
<https://doi.org/10.3311/PPee.14237>

[25] Dekali, Z., Baghli, L., Boumediene, A. "Indirect power control for a Grid Connected Double Fed Induction Generator Based Wind Turbine Emulator", In: 2019 International Conference on Advanced Electrical Engineering (ICAEE), Algiers, Algeria, 2019, pp. 1–6.  
<https://doi.org/10.1109/ICAEE47123.2019.9014778>

[26] Almakki, A. J., Mazalov, A. "Improved DFIG DFTC by Using a Fractional-Order Super Twisting Algorithms in Wind Power Application", *Modern Transportation Systems and Technologies*, 7(3), pp. 131–149, 2021.  
<https://doi.org/10.17816/transsyst202173131-149>

[27] El Amine, B. B. M., Ahmed, A., Houari, M. B., Mouloud, D. "Modeling, simulation and control of a doubly-fed induction generator for wind energy conversion systems", *International Journal of Power Electronics and Drive System (IJPEDS)*, 11(3), pp. 1197–1210, 2020.  
<https://doi.org/10.11591/ijpeds.v11.i3.pp1197-1210>

[28] Munisamy, V., Vadivoo, N. S., Devasena, V. "Stochastic Distribution Controller for Wind Turbines with Doubly Fed Induction Generator", *Distributed Generation & Alternative Energy Journal*, 35(4), pp. 307–330, 2021.  
<https://doi.org/10.13052/dgaej2156-3306.3544>

[29] Azza, A., Kherfane, H. "Robust Control of Doubly Fed Induction Generator Using Fractional Order Control", *International Journal of Power Electronics and Drive Systems (IJPEDS)*, 9(3), pp. 1072–1080, 2018.  
<https://doi.org/10.11591/ijpeds.v9.i3.pp1072-1080>

## Appendix

**Table 4** Wind turbine parameters

|                                                |                           |
|------------------------------------------------|---------------------------|
| Gearbox ratio (G)                              | 5.4                       |
| Number of blades Blade radius (R)              | 3 m                       |
| Nominal wind speed (v)                         | 16 m/s                    |
| Moment of inertia (J)                          | 0.2 Kg m <sup>2</sup>     |
| Viscous friction coefficient (f <sub>r</sub> ) | 0.003 N m s <sup>-1</sup> |

**Table 5** Doubly Fed Induction Generator parameters

|                                        |           |
|----------------------------------------|-----------|
| Number of pairs of poles (p)           | 2         |
| Rated power (P <sub>n</sub> )          | 4 KW      |
| Stator rated frequency (f)             | 50 Hz     |
| Stator rated voltage (V <sub>s</sub> ) | 220/380 V |
| Stator inductance (L <sub>s</sub> )    | 0.1554 H  |
| Rotor inductance (L <sub>r</sub> )     | 0.1568 H  |
| Mutual inductance (L <sub>m</sub> )    | 0.15 H    |
| Stator inductance (R <sub>s</sub> )    | 1.2 Ω     |
| Rotor inductance (R <sub>r</sub> )     | 1.8 Ω     |